Citation: CPT Pharmacometrics Syst. Pharmacol. (2016) 5, 505–515; doi:10.1002/psp4.12110

TUTORIAL

Quantitative Prediction of Drug–Drug Interactions Involving Inhibitory Metabolites in Drug Development: How Can Physiologically Based Pharmacokinetic Modeling Help?

IE Templeton[1]*, Y Chen[1], J Mao[1], J Lin[2], H Yu[3], S Peters[4], M Shebley[5] and MV Varma[2]*

This subteam under the Drug Metabolism Leadership Group (Innovation and Quality Consortium) investigated the quantitative role of circulating inhibitory metabolites in drug–drug interactions using physiologically based pharmacokinetic (PBPK) modeling. Three drugs with major circulating inhibitory metabolites (amiodarone, gemfibrozil, and sertraline) were systematically evaluated in addition to the literature review of recent examples. The application of PBPK modeling in drug interactions by inhibitory parent–metabolite pairs is described and guidance on strategic application is provided.
CPT Pharmacometrics Syst. Pharmacol. (2016) **5**, 505–515; doi:10.1002/psp4.12110; published online 19 September 2016.

OVERVIEW

Drug–drug interactions (DDIs), associated with altered drug clearance, are a major source of severe adverse reactions and drug withdrawals.[1–3] For this reason, predicting and managing the impact of DDIs, involving cytochromes P-450 (CYPs) and other drug-metabolizing enzymes, have long been emphasized in drug discovery and development.[4] In addition, the clinical implications of transporter-based DDIs have recently been highlighted.[5–8] Mechanisms involved in DDIs that affect enzyme activity can be broadly categorized as reversible inhibition, mechanism-based (irreversible) inhibition, and induction. Generally, the parent drug is the only or primary perpetrator species responsible for the observed DDI. However, the potential contribution of metabolite(s) circulating at high levels in the blood has been recently debated.[9] There are now noted examples where circulating metabolites may have partially or fully contributed to the observed clinical DDIs.[9–13] As a result, recent regulatory guidance recommends investigation of the role of metabolites in clinical DDIs. Specifically, both the European Medical Agency (EMA) and US Food and Drug Administration (FDA)[14,15] have proposed criteria based on the relative exposure of metabolite and parent drug in systemic circulation. Sponsors are encouraged to investigate the *in vitro* interaction potential of a metabolite when that metabolite is present at $\geq$25% of parent area under the plasma concentration–time curve (AUC) (FDA) or $\geq$25% of parent AUC and $\geq$10% of total drug-related AUC (EMA).

PBPK modeling and simulation is a computer-based approach that permits a quantitative mechanistic description of systemic drug exposure. Increased application of PBPK in the drug discovery and development settings is now evident.[16] A PBPK model is a mathematical model that is developed based on available data and the overall objective of the modeling effort. Broadly, application of PBPK may be grouped into three general categories: so-called "top-down," "bottom-up," and "middle-out" approaches. A top-down approach refers to the more traditional fitting of models to observed clinical data. Bottom-up models are typically created at earlier stages of drug development and, as such, rely primarily on a combination of *in vitro* and *in silico* data. Middle-out models incorporate both *in vitro* and *in vivo* data while also leveraging "learn and confirm" cycles of feedback and model optimization.

In order to evaluate the application of the guidance documents in drug development, the Metabolite-Mediated DDI Scholarship Group (MDSG) was formed under the umbrella of the Drug Metabolism Leadership Group of the Innovation and Quality Consortium (IQ-DMLG). The MDSG conducted a thorough literature review of *in vitro* and *in vivo* DDIs for 137 most-frequently prescribed drugs. The objectives of this scholarship group were: first, to understand the frequency of cases where metabolite(s) significantly contributed to DDIs, and second, to assess current practices for metabolite *in vitro* inhibition studies in drug development settings.[12] Of the DDIs reviewed by the MDSG, several drugs (including gemfibrozil, sertraline, bupropion, and amiodarone) were identified with "surprise" DDIs: examples in which *in vivo* CYP inhibition was not predicted by *in vitro* CYP inhibition data. For these examples, metabolites were proposed to contribute to the *in vivo* CYP inhibition. The MDSG was subsequently interested in investigating possible strategies (i.e., PBPK) that can prospectively prompt the assessment of CYP inhibition potential of metabolites in order to avoid "surprise" clinical DDIs due to metabolites.

To further assess the quantitative contribution of circulating metabolite(s), a Metabolite Scholarship PBPK Modeling subteam was formed. This team was composed of scientists representing IQ member pharmaceutical companies

[1]Genentech, South San Francisco, California, USA; [2]Pfizer Inc., Groton, Connecticut, USA; [3]Boehringer Ingelheim Pharmaceuticals, Ridgefield, Connecticut, USA; [4]AstraZeneca, Mölndal, Sweden; [5]AbbVie Inc., North Chicago, Illinois, USA. *Correspondence to: IE Templeton or MVS Varma (templeton.ian@gene.com or manthena.v.varma@pfizer.com)
Received 16 June 2016; accepted 8 August 2016; published online on 19 September 2016. doi:10.1002/psp4.12110

with expertise in PBPK modeling and simulations. Here we present the position of the Metabolite Scholarship PBPK modeling team in the application of mechanistic modeling approaches to predict and/or rationalize the role of circulating metabolites in observed clinical DDIs. We have summarized the current state of the science and reviewed select case examples of perpetrator drugs with inhibitory metabolites. Based on the learnings from these examples, pragmatic guidance is proposed for implementing mechanistic modeling to facilitate decision making at different stages of development.

MECHANISTIC CONSIDERATIONS AND PREDICTION OF INHIBITORY METABOLITE EXPOSURE

The metabolite-to-parent exposure in the blood (also referred to as AUC_m/AUC_p) after the intravenous or oral administration of parent is expressed by Eqs. 1 and 2, respectively[17,18]:

$$\frac{AUC_m}{AUC_p} = \frac{f_m \cdot CL_p}{CL_m} \quad (1)$$

$$\frac{AUC_m}{AUC_p} = \frac{f_m \cdot CL_p}{F_h \cdot CL_m} \quad (2)$$

where CL_p and CL_m are the total *in vivo* clearances of the parent and metabolite, respectively. Other critical parameters include the fraction of parent metabolized to form the particular metabolite (f_m) and the fraction of parent escaping hepatic first-pass extraction (F_h). It is therefore apparent that major circulating metabolites are generally a result of high formation clearance ($f_m \cdot CL_p$) and/or low elimination clearance (CL_m). Intuitively, one would expect that estimation of these parameters could facilitate identification of major circulatory metabolites, which would then need further characterization for interaction potency. However, metabolite disposition is often complicated by a lack of understanding of the multiple processes that define formation and elimination clearances, or of metabolite availability at the site of interaction relevant for DDIs.

Following oral administration of the perpetrator parent drug, metabolite(s) may be formed in the enterocytes during intestinal first-pass extraction by a range of drug metabolizing enzymes, including CYPs (**Figure 1**). The CYP3A family (e.g., CYP3A4 and CYP3A5) is the predominant CYP family in the small intestine, accounting for about 80% of total CYP content in this organ.[19,20] Although the abundance of CYP3A4 in the intestine accounts for only 1% of the average CYP content in the liver,[20,21] intestinal metabolism has been observed to contribute more to first-pass extraction, to a significant extent, compared to hepatic metabolism for certain drugs.[22–26] Intestinal metabolism may result in availability of metabolite(s) within the enterocytes, which could inhibit the metabolism and/or active efflux transport at the site (**Figure 1**). Additionally, metabolites are generally more hydrophilic than the parent drug, which may limit passive permeability and result in higher enterocyte concentrations of metabolites compared to parent.[27] Metabolite(s) formed in the enterocytes may subsequently be transported into the blood or intestinal lumen via efflux transporters such as P-glycoprotein (P-gp), breast cancer resistant protein (BCRP), and multidrug resistant proteins (MRPs).[28] For example, the metabolite of ropivacain is secreted into intestinal lumen to a larger extent compared to parent.[29] Parent and the metabolite formed in enterocytes and available in portal blood may also contribute to the inhibition of hepatic uptake transporters such as organic anion transporting polypeptides (OATP)1B1 and OATP1B3 and organic cation transporter 1 (OCT1).

The relationship between plasma concentration of parent and metabolites, which is readily measurable, and exposure at the site of interaction, which is not, is another complicating factor. It is often assumed that the drug concentration at the site of interaction (e.g., liver inlet for uptake transporters and hepatocyte cytosol for the enzymes and biliary efflux transporters) is similar to the unbound drug concentration at the plasma/blood sampling site. However, this is not always the case. Depending on the hepatic extraction, concentration of parent and metabolite in the inlet of the liver could be significantly higher than concentrations observed in venous blood. On the other hand, free liver concentrations of the parent and metabolite at steady-state could differ from the free blood concentration due to involvement of drug transporters. Several uptake transporters including OATPs, sodium taurocholate cotransporting polypeptide (NTCP), OCT1 and organic anion transporter 2 (OAT2), are expressed on the sinusoidal membrane of hepatocytes, as well as the efflux pumps, MRP3 and MRP4.[28] Additionally, canalicular efflux transporters (P-gp, BCRP, and MRP2) may contribute to the biliary elimination. For example, plasma and liver exposure of gemfibrozil 1-*O*-β-glucuronide, the major circulating metabolite of gemfibrozil, is determined by uptake (OATPs) and efflux transporters (MRPs).[30,31]

Finally, renal clearance involving glomerular filtration and active secretion is important in the clearance of hydrophilic oxidative or conjugated metabolites. Overall, the enzyme-transporter interplay at the intestine and liver, and the contribution of active and passive renal clearance, determines the disposition or concentration of parent and metabolites at the relevant site of interaction. Therefore, each of these processes, and their relative roles, must be well understood in order to predict the exposure of the parent and metabolite perpetrating the clinical DDIs. Due to limited tools and key knowledge gaps in the translation of several nonenzymatic processes, prospective prediction of metabolite exposure at the site of interaction is highly challenging.

MODEL-BASED APPROACHES FOR PREDICTING DDIs CAUSED BY INHIBITORY METABOLITES

Mathematical models may be broadly grouped into descriptive categories: simple static, mechanistic static, dynamic minimal-PBPK, and full PBPK models.[16] These represent a spectrum of increasingly parameterized models, which rely

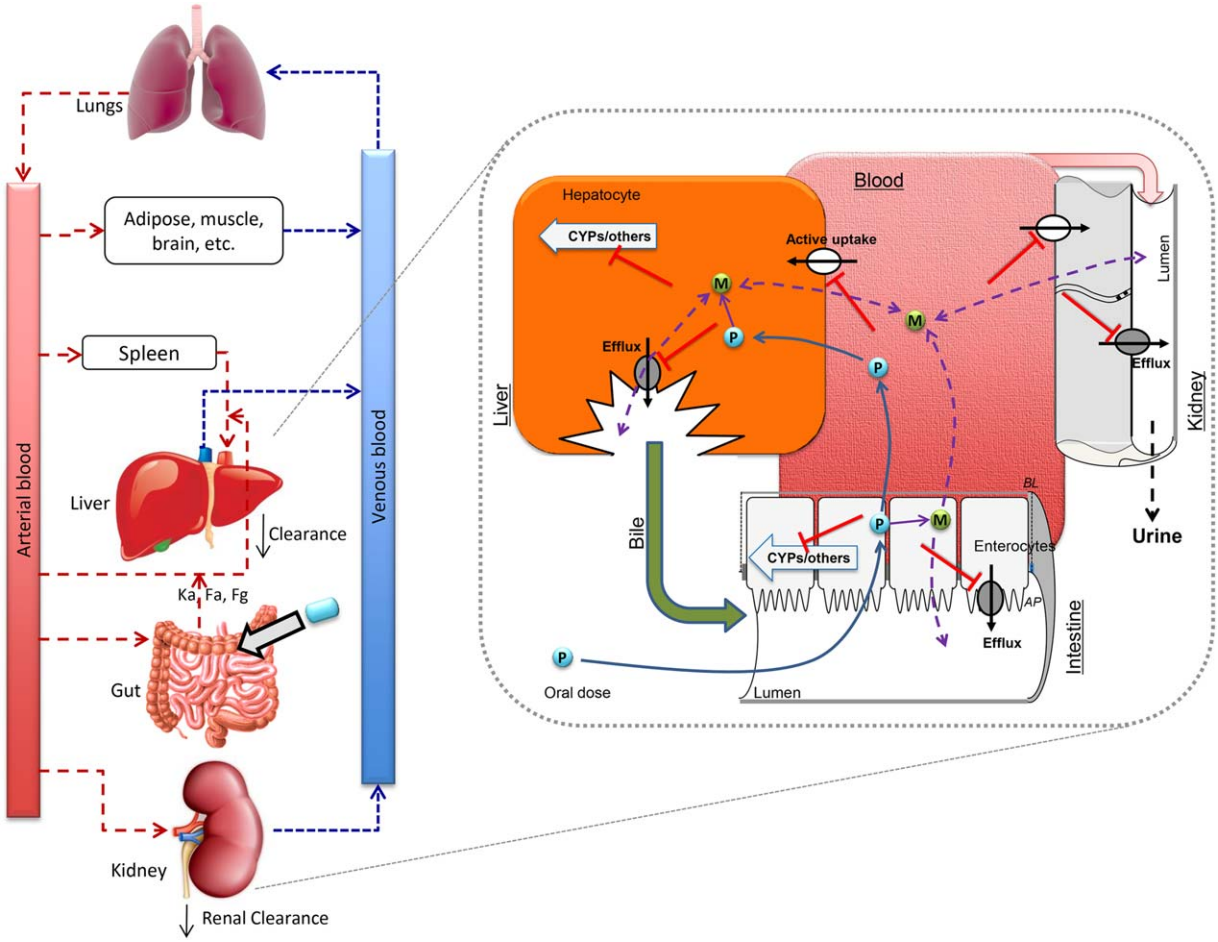

Figure 1 Mechanistic framework for the prediction of DDIs involving inhibitory metabolites. Intestine and liver are the major sites of drug interactions, and concentrations of the parent and metabolites at the site of interaction is determined by enzyme–transporter interplay in these organs. Hydrophilic metabolites are also cleared in the urine by active and passive processes. P, parent; M, metabolite.

upon an increasing number of accompanying assumptions and required experimental inputs.

Simple and mechanistic static models

The simple static and mechanistic static models for parent drug have been well elaborated in FDA and EMA guidance documents.[14,15] These models may be adapted by adding the elements of inhibitory metabolites for the prediction of clinical DDIs, which involve perpetrator parent drugs with known inhibitory metabolites (**Table 1**). The most basic (i.v. drug administration) model for the estimation of DDIs is the static prediction of change in victim drug AUC as a function of inhibition potency (K_i) and perpetrator exposure in the liver (I_H) for both parent and circulating metabolite (Eq. 3)[11,13]:

$$\frac{AUC^{inhibited}}{AUC} = 1 + \left(\frac{[I_{H,parent}]}{K_{i,parent}} + \frac{[I_{H,metabolite}]}{K_{i,metabolite}} \right) \quad (3)$$

In the most basic static models, prediction of DDI magnitude is driven by a single unbound perpetrator concentration. There is considerable debate in the literature regarding selection of relevant *in vivo* perpetrator concentration estimates used in the static model (e.g., average systemic (I_{av}), maximum systemic (I_{max}), or hepatic inlet (I_{inlet})).[4,32,33]

Typically, basic models are applied to project a worst-case scenario in situations where prior knowledge (experimental data) is limited. Prior to the availability of clinical exposure data, estimation of perpetrator concentration in human may be based on the prediction from preclinical data and desired efficacious exposure. In order to investigate the role of metabolites, application of static DDI models require an understanding of metabolite concentrations as well. Although the mechanistic static models are limited to predictions based on single inhibitor concentrations, models provide a more realistic estimate of DDI risk by incorporating additional factors such as the interaction at the level of intestine (for an orally administered drug), parallel routes of elimination for the victim drug, and transporter–enzyme interplay.[4,34–38] There are several variations of models with increasing complexity reported in the literature and subsequently summarized in the 2012 FDA draft DDI guidance.[14] The mechanistic static model suggested by the 2012 draft FDA guidance was based on the original equations published by Rowland *et al*.[39] Subsequently, this approach was modified by others[32,35,40] and is regularly

Table 1 Summary of available DDI modeling approaches commonly applied in drug development

Approach	Inhibitor concentrations [I]	Strengths	Limitations
Simple Static	Total or unbound observed or predicted for both the parent and inhibitory metabolite(s) (I_{ave}, I_{inlet}, I_{max})	• Limited input data required	• Very simplified often resulting in a conservative estimate • Liver DDI only • Does not capture parallel clearance and elimination pathways • Lacks physiology inputs
Mechanistic Static	Total or Unbound observed or predicted for both the parent drug and inhibitory metabolite(s) (I_{ave}, I_{inlet}, I_{max})	• Limited input data required • Description of parallel clearance and elimination pathways • Ability to incorporate DDI at the level of intestine • Can capture transporter-mediated disposition	• Lack consideration to time-varying perpetrator concentration • Assume linear PK and does not consider accumulation
Minimal-PBPK	Simulation based on pharmacokinetic and physiology data for both the parent drug and inhibitory metabolite(s)	• Description of parallel clearance and elimination pathways • Can capture transporter-mediated disposition	• Typically includes liver, gut with other tissues lumped into a virtual "systemic compartment"
Full PBPK	Simulation based on pharmacokinetic and physiology data for both the parent drug and inhibitory metabolite(s)	• Thorough physiology description • Description of parallel clearance and elimination pathways • Can capture transporter-mediated disposition • Application in special populations	• Requires extensive *in vitro* and *in vivo* data or *in silico* predicted parameters

used in DDI risk assessment. Further modifications can allow for incorporation of multiple inhibitory species, including metabolites (Eq. 4):

$$\frac{AUC^{inhibited}}{AUC} = \left(\frac{1}{(1-F_G)\times\left(\frac{1}{1+\left(\frac{[I_{G,parent}]}{K_{i,parent}}\right)}\right)+F_G}\right) \times \left(\frac{1}{f_{m.CYP}\times\left(\frac{1}{1+\left(\frac{[I_{H,parent}]}{K_{i,parent}}+\frac{[I_{H,metabolite}]}{K_{i,metabolite}}\right)}\right)+(1-f_{m.CYP})}\right) \quad (4)$$

Here, F_G is the relative fraction of substrate escaping first-pass extraction in the gut and $f_{m,CYP}$ is the relative contribution of the inhibited CYP to the overall metabolic clearance of the drug. The parameter F_G will be important when considering interactions with CYP enzymes abundant in the gut (e.g., CYP3A4). Various methods have been utilized to predict the required parameters (F_G and $f_{m,CYP}$) based on *in vitro* data (i.e., estimated intestinal blood flow as a function of permeability Q_{gut} and *in vitro* phenotyping[26,41]). A much more detailed summary of approaches used to characterize $f_{m,CYP}$ was recently published by another DMLG working group.[42] In guidance documents, regulatory agencies suggested a worst-case scenario prediction of intestinal drug concentration (I_g) based on the ratio of molar dose amount to a hypothetical intestine lumen volume of 250 mL. This approach assumes instant and complete dissolution of the complete dose, ignoring solubility and membrane permeability factors and is likely to be an overprediction of actual luminal concentration in many cases, specifically BCS class II and IV compounds. A more mechanistic approach was suggested that requires an understanding of fractional absorption (F_a), absorption rate (k_a), and estimated enteric blood flow ($Q_{enteric}$) (Eq. 5) and assumes minimal extraction drug dose (D) by first pass metabolism[43]:

$$I_G = \frac{F_a \times k_a \times D}{Q_{enteric}} \quad (5)$$

Minimal- and full-PBPK dynamic models

PBPK models integrate compound-related data, along with species physiology, to simulate the change of drug exposure in plasma and tissue. Minimal-PBPK models incorporate select physiological parameters, including blood flows, tissue volumes, etc., and are generally focused on organs with critical impact on *in vivo* drug disposition (such as liver and intestine), while lumping other organs (i.e., well-perfused) into a single virtual compartment.[44] While this is appropriate for some drugs, which exhibit one-compartment PK, minimal models may require an additional compartment to represent distribution into poorly perfused organs. Full PBPK models additionally incorporate sophisticated physiological information that accounts for mass/drug transfer between physiological compartments, along with mechanistic models for absorption, metabolism, distribution, and elimination and often consider population variability (**Figure 1**).[45] PBPK models allow for a more mechanistic estimation of inhibitor concentration (metabolite and/or parent) at the site of DDI in the relevant organ(s) compared to simplified models (e.g., the static models). One of the primary advantages of the PBPK approach for DDI prediction for parent drugs with known inhibitory metabolites is that it can describe formation of inhibitory metabolite(s) quantitatively from parent clearance. This is of particular interest in cases where the relationship between parent and metabolite concentration in systemic circulation is time- or dose-dependent. This approach may decrease the number of false-positive predictions or support the design of more informative clinical DDI studies.

Table 2 Summary of *in vitro* inhibition potency and observed and predicted *in vivo* DDIs for case studies

		K_i (μM)			Observed AUCR			
Parent	Metabolite	Transporter/ enzymes	Parent	Metabolite	Co-Med	AUCR	Predicted AUCR	Key learnings
Amiodarone	MDEA	CYP2C9,	94.6	2.3	warfarin	1.27–1.73	1.18	No interaction was predicted without considering inhibitory metabolite. PBPK modeling revealed possible mechanism of clinical observed AMIO DDIs[41]
		CYP2D6,	45.1	4.5	metaprolol	2.11	2.45	
		CYP3A4	271.6	12.2	simvastatin	1.97	1.93	
Gemfibrozil	Gem-Glu	OATP1B1 and CYP2C8	2.54	7.9	Repaglinide	5-8	5.9	No significant interactions were predicted without considering inhibitory metabolite. PBPK modeling considering transporter and enzyme inhibition better predicted clinical DD observations. Metabolite contributed majorly to the observed DDIs[21]
		CYP2C8	6.9	(7.9 μM and 12.6h^{-1})[a]	Rosiglitazone	2.8	2.5	
Sertraline	NDMS	CYP2D6	0.16[b]	0.46[b]	desipramine	1.54	1.08	Consideration of parent and metabolite inhibition potential predicted lack of CYP2D6 DDI. Considering inhibition potential of parent alone predicted the risk of clinical CYP3A DDI
		CYP3A	0.22[b]	0.11[b]	pimozide	1.37	1.83	

[a]K_i corrected for microsomal binding.
[b]Time-dependent inhibition of CYP2C8 by gemfibrozil 1-O-β-glucuronide – values represent K_I corrected for binding to microsomal protein and k_{inact}, respectively.

PBPK modeling and simulation of DDI involving inhibitory metabolite: case examples

Three case examples were investigated by this subgroup. Amiodarone and gemfibrozil examples have been published individually in greater detail by members of this subgroup.[31,46] A high-level summary of amiodarone and gemfibrozil investigations, along with a description of the investigation of sertraline, is provided below. In the following three case examples, we summarize the PBPK modeling applied to describe the role of inhibitory metabolites in observed clinical DDIs. In addition, guidance is provided for strategic application of mechanistic modeling in situations where metabolites may potentially contribute to clinical DDI. *In vitro* inhibition parameters, and observed and predicted *in vivo* DDIs using developed PBPK models, are summarized in **Table 2.**

Amiodarone. Amiodarone (AMIO) is an effective antiarrhythmic agent with documented clinical DDIs with comedications, including simvastatin (AUC increased by 1.7-fold), dextromethorphan (1.3–2-fold), and warfarin (1.2–2-fold) at therapeutic doses of AMIO (200–400 mg).[47–49] These clinically observed DDIs were not expected based on AMIO *in vitro* competitive inhibition data (K_i >45 μM for all CYPs).[50] However, *in vitro* studies imply that the AMIO metabolite, mono-desethyl-amiodarone (MDEA), is a more portent inhibitor, with K_i values of 2.3 μM, 4.5 μM, and 12.1 μM for CYP2C9, CYP2D6, CYP3A4, respectively.[50,51] Considering that MDEA is a major metabolite with plasma exposure comparable to the parent after chronic treatment (~1–5 μM at steady-state), it was hypothesized that MDEA may play an important role in the observed inhibition DDI.

A PBPK model was developed using a mixed "bottom-up" and "top-down" approach (i.e., "middle-out") to simulate the pharmacokinetic profile of both AMIO and MDEA.[46] In order to obtain the mechanistic understanding of how MDEA could contribute to the clinically observed AMIO DDIs, particular emphasis of the PBPK modeling was placed on predicting the accumulation of both parent and metabolite in plasma and liver after multiple doses.[46] This is especially important for AMIO, as it is used as a chronic therapy. Key PBPK model parameters (clearance and volume of distribution) for both AMIO and MDEA, and formation kinetics for MDEA after i.v. administration of AMIO, were defined using a combination of *in silico*, *in vitro*, and *in vivo* data.[46] Simulations of AMIO and MDEA pharmacokinetic profiles, after single and multiple oral doses, were performed as a verification of the PBPK model developed using i.v. pharmacokinetic data. The AMIO-MDEA linked PBPK model predicted both the formation and elimination of MDEA successfully based on comparison of the observed and simulated MDEA pharmacokinetic profiles.[46] More important, the observed accumulation of AMIO and MDEA in plasma and liver after chronic oral dosing was well described by the simulations. At steady-state, the simulated plasma concentration of metabolite MDEA reached levels similar to the parent AMIO (~1 μg/mL), consistent with clinical observations.[51,52] The DDIs between AMIO and substrates warfarin (CYP2C9), metoprolol (CYP2D6), and simvastatin (CYP3A4) were then simulated using the established model; all plausible mechanisms of CYP inhibition by AMIO and its metabolite MDEA were considered.

In general, incorporation of the inhibitory metabolite MDEA into the PBPK model resulted in more accurate predictions of all DDIs compared to the predictions based on the parent alone. These simulations led to increased confidence in the hypothesized mechanism of the DDI caused by AMIO. The observed AMIO–metoprolol interaction was attributed to the TDI of CYP2D6 mediated by MDEA. The AMIO–simvastatin interaction was associated with competitive inhibition by both parent and metabolite. Finally, the observed DDI with warfarin was dependent on incorporation

of additional AMIO metabolites (DDEA, ODAA) recently identified as more potent CYP2C9 inhibitors.[51] Overall, this work demonstrated the utility of "middle-out" PBPK modeling in improving the mechanistic understanding of the observed clinical DDI. Through simulation of the proposed mechanism of inhibition, the disconnect between the initial DDI predictions and observed data was explained by the contribution of a major circulating inhibitory metabolite.[46]

Gemfibrozil. Gemfibrozil is often prescribed and is generally a well-tolerated drug for the treatment of patients with elevated serum triglyceride levels and for reducing the risk of coronary heart disease.[53] Gemfibrozil is known to perpetrate various drug interactions. However, the major indication of its severe interaction potential emerged with cerivastatin as a victim drug. Higher incidence of fatal rhabdomyolysis was linked to increased cerivastatin exposure in patients on gemfibrozil.[54,55] Other notable gemfibrozil DDIs involve victim drugs repaglinide (AUC ratio (AUCR) $\sim$8),[56,57] pioglitazone (AUCR $\sim$4),[58] and rosiglitazone (AUCR $\sim$2.5).[59] Subsequently, cerivastatin was withdrawn from the market, and the concomitant use of gemfibrozil and repaglinide is contraindicated.[57] On the basis of these clinical data, gemfibrozil has been suggested as a strong CYP2C8 inhibitor for clinical investigation by both the FDA and the EMA.[14]

Gemfibrozil presents a complex interaction profile involving inhibition of multiple transporters and CYP2C8 by parent and its metabolite, gemfibrozil 1-O-β-glucuronide (Gem-Glu). Gem-Glu is a TDI of CYP2C8; both parent and metabolite also behave as moderate inhibitors of OATP1B1, OAT3, and weakly inhibit CYP2C9 and CYP3A4.[60–62] A PBPK model for gemfibrozil, incorporating relevant data to capture Gem-Glu pharmacokinetics and interaction mechanisms, was developed.[31] The primary objectives were to understand the quantitative role of Gem-Glu in the magnitude of gemfibrozil DDIs and to assess the ability of the PBPK modeling approach to predict complex drug interactions involving transporter–enzyme interplay and multiple inhibitory species.[31] The multiple interaction mechanisms (CYP2C8 and OATP1B1) of both parent and metabolite are simultaneously implemented in the PBPK model to predict DDIs of representative victim drugs including cerivastatin, pioglitazone, repaglinide, and rosiglitazone. While consideration of parent alone led to a significant underprediction, the inclusion of Gem-Glu in the PBPK model greatly improved the accuracy of predicted AUC ratios and plasma concentration–time profiles of victim drugs.

Model-based simulations suggest that Gem-Glu has a much larger inhibitory effect than that of the parent *in vivo,* due to its relatively higher unbound concentrations and CYP2C8 potency. Sensitivity analyses on the impact of metabolite-to-parent ratio on AUCR suggested that Gem-Glu exposure at $\sim$10% of the parent moved the DDI category from no or weak (AUCR $<$2) to moderate (2 $<$ AUCR $<$ 5) for all four victim drugs.[31] This suggests that the Gem-Glu exposure that is needed to bring about complete inactivation of CYP2C8 is only a fraction of that achieved in the clinic following a 600 mg b.i.d. gemfibrozil dose. The regulatory recommendation to trigger *in vitro* investigation of interaction potential of metabolites applies to Gem-Glu due to its systemic exposure being $\geq$25% of parent AUC. However, the TDI component makes the metabolite a major perpetrating species for CYP2C8 inhibition even when available at $<$10% of parent AUC. Furthermore, the DDI risk *in vivo* when metabolites inhibit both uptake transport and metabolism is expected to be large. Overall, the default metabolite-to-parent exposure cutoff ($\geq$25%) may not firmly reflect upon the DDI potential following gemfibrozil dosing. Collectively, the gemfibrozil case study reinforces the utility of *in vitro* data and the modeling approaches that mechanistically integrate the multiple components in the DDI risk assessment. Furthermore, transporter–enzyme interplay and the role of perpetrator metabolites need to be carefully considered to achieve quantitative rationalization and/or prediction.

Sertraline. Sertraline is a selective serotonin reuptake inhibitor (SSRI), which is now a highly prescribed antidepressant and psychiatric medication. Sertraline undergoes extensive metabolism, with the major circulating metabolite being N-desmethyl-sertraline (DMS), which is pharmacologically less active than sertraline. Although multiple CYPs (CYP2D6, CYP2C9, CYP2B6, CYP2C19, and CYP3A4) are responsible for the metabolism of sertraline, CYP2C19 is the principal drug metabolizing enzyme contributing to N-demethylation.[63–65] Under steady-state conditions, DMS concentrations in plasma are higher than that of sertraline. The ratio of DMS to sertraline vary from 1.1–4.1-fold among the patients receiving sertraline at 100–300 mg/day (Pfizer internal data). Both sertraline and DMS are weak CYP2D6 inhibitors. Clinical studies demonstrated an increase in AUC of CYP2D6 probe substrate desipramine by $\sim$50%.[66] Sertraline is also a weak competitive inhibitor of CYP3A and has been reported to increase the plasma concentration of pimozide, a drug mainly metabolized by CYP3A4.[67]

A PBPK model was developed for sertraline and DMS, where the sertraline model was built "bottom-up" and the metabolite model was developed with a "middle-out" approach; .25; metabolite model input parameters were acquired from both *in vitro* studies and observed clinical pharmacokinetics (**Supplementary Table 1**). The final PBPK model recovered plasma concentration–time profiles of both sertraline and DMS following single and multiple doses of sertraline (**Figure 2**). A SimCYP default model (v. 14, Cetara) of the victim drug desipramine was used to assess CYP2D6-mediated DDIs (**Supplementary Dataset 1**). Additionally, a desipramine model was verified for its utility to assess CYP2D6-mediated interactions based on the predictability of the interaction with paroxetine as perpetrator drug (observed vs. predicted AUC ratios are 5 and 5.8, respectively). Using this verified desipramine model, no DDI was predicted when coadministered with a single 150 mg dose of sertraline (**Figure 2**). Furthermore, no DDI was predicted with multiple doses of sertraline (150 mg, 8 doses), where the predicted value was only 1.08 and the mean observed AUC ratio was 1.54 (**Table 2**). No significant difference in prediction accuracy was observed when metabolite (DMS) interaction potency was included. The lack of predicted DDI with the parent–metabolite pair suggests the possibility that other interaction mechanisms, not

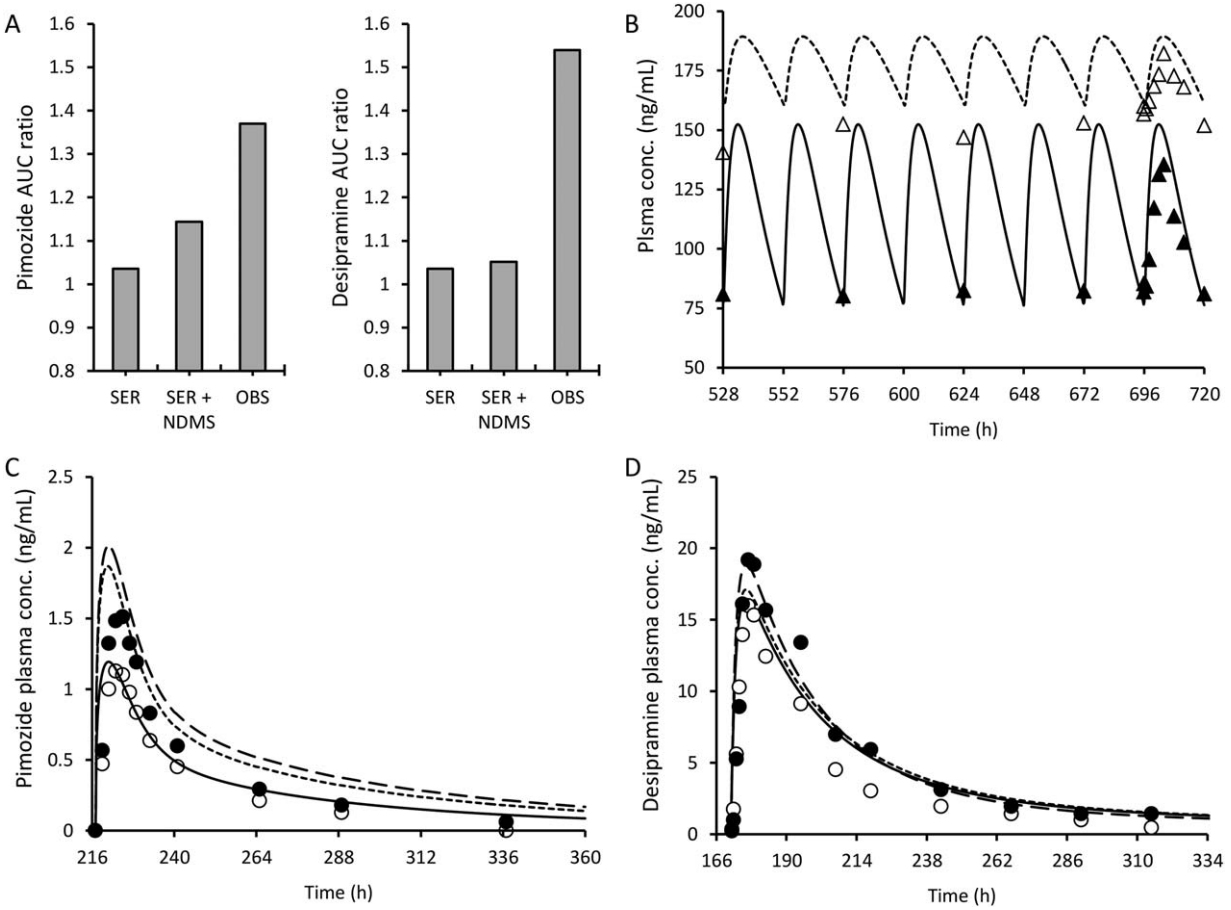

Figure 2 Model-based prediction of sertraline DDIs. (**a**) Static model ($1+I_{max,u}/IC_{50}$) based prediction of pimozide (CYP3A substrate) and desipramine (CYP2D6 substrate) interactions when assuming sertraline alone or in combination with metabolite, NDMS, as the perpetrator species. (**b**) PBPK model simulation of the plasma concentration–time profiles of sertraline (closed triangles) and its metabolite (open triangles) following multiple oral dose of sertraline. (**c**) PBPK model prediction of pimozide-sertraline DDI. (**d**) PBPK model prediction of desipramine-sertraline DDI. Plots c and d, data points represent observed data in the absence (open circles) and presence of sertraline dose; and the curves represent model prediction of control (solid curve), in the presence of sertraline alone (dotted curves) and in the presence of sertraline and NDMS. PBPK model input parameters are provided in **Supplementary Table 1**.

currently fully understood, are needed to be captured in the mechanistic modeling (for example, TDI of CYP2D6) and may need further investigation.

Using a simple static model (i.e., maximum free inhibitor concentration in plasma divided by K_i), sertraline as a perpetrator was categorized as "no risk" for CYP3A4-mediated interactions when assuming parent as the lone interacting species, as well as when the parent–metabolite pair was considered (predicted AUC ratio <1.25). However, to mechanistically assess the CYP3A-mediated interactions and rationalize the observed pimozide–sertraline clinical interaction, a PBPK model was developed for pimozide, which is primarily metabolized by CYP3A4 with a minor role of CYP1A2.[68] The pimozide model (**Supplementary Dataset 2**) was verified using clinical pharmacokinetic data and further validated by simulating its clinical interaction with the CYP3A inhibitor, clarithromycin (observed vs. predicted AUC ratios are 2.1 and 2.5, respectively).[69] The sertraline model (parent alone) predicted a mean 57% increase in AUC of pimozide compared to the clinically observed 37% increase following 200 mg daily dose for 29 days (Pfizer data on file). However, the model predicted an 83% increase in pimozide AUC when inhibition by both sertraline and DMS was considered. The difference of lack of interaction with the simple static model vs. significant interaction using the PBPK model is due to the mechanistic consideration of CYP3A inhibition by sertraline at the gut. Overall, unlike the case examples of amiodarone and gemfibrozil, the sertraline mechanistic modeling suggests that consideration of the major circulating metabolite does not explain the modest CYP3A and CYP2D6 interactions observed in the clinic, and implies the need to further investigate the unknown mechanisms.

STRATEGIES FOR PREDICTING DDI INVOLVING INHIBITORY METABOLITES

Of more than 100 drugs previously assessed using static models, amiodarone, bupropion, gemfibrozil, and sertraline

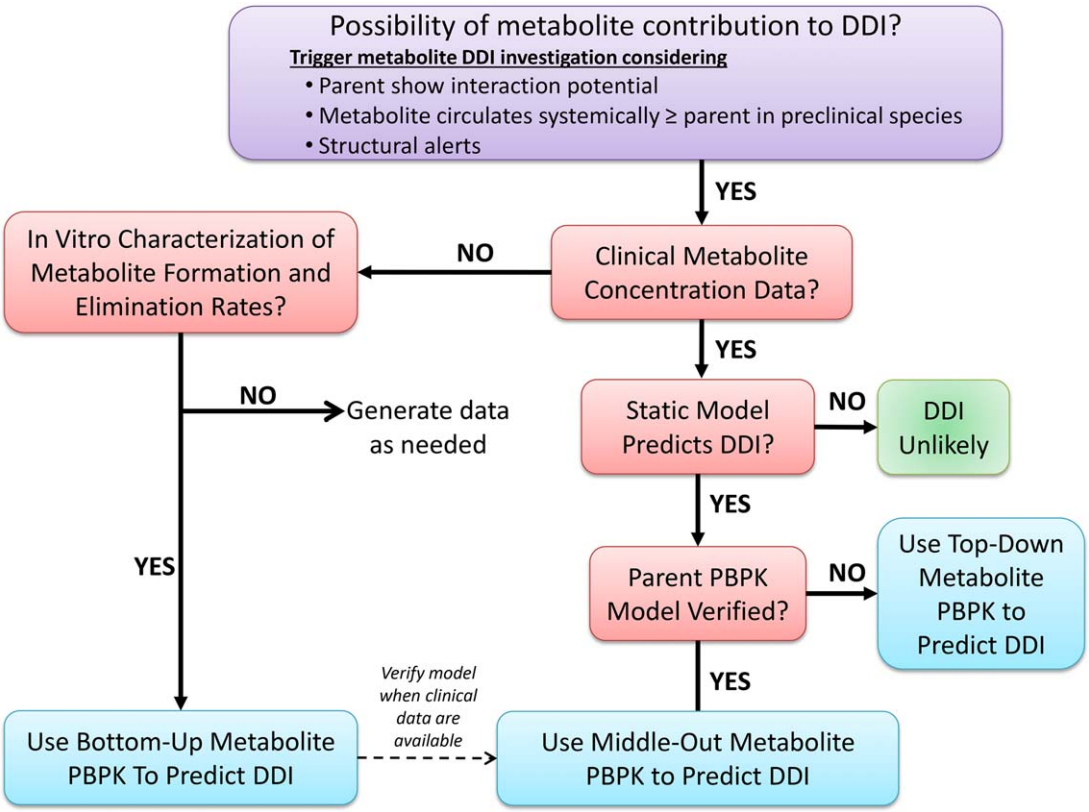

Figure 3 A mechanistic modeling strategy to prospectively predict DDIs involving inhibitory metabolites. Trigger metabolite inhibition potential characterization if the parent is an inhibitor and the metabolite exposure is predicted or observed to be equal of more than parent exposure with some considerations to the structural alerts for possible enzyme inhibition.[12] Top-down metabolite models leverage observed *in vivo* metabolite data with minimal integrated mechanistic information. In this approach, the metabolite PBPK model relies on optimization, which is dependent on high confidence in the parent PBPK model. Top-down models rely on fitting the clinical concentration time data for the parent and metabolites. Bottom-up models must be applied in cases where *in vivo* data for the metabolite are not yet available. This approach relies on *in vivo* parent data and *in vitro* metabolites data (formation and elimination rate) and established *in vitro/in vivo* extrapolation (IVIVE). Once *in vivo* metabolite concentration data are available, a middle-out approach may be applied. Finally, middle-out models are developed based on a combination of observed *in vivo* metabolite concentration data and *in vitro* information of the mechanisms driving *in vivo* metabolite exposure. The middle-out approach allows for the greatest level of confidence in the utility of the metabolite PBPK model based on this understanding of the underlying mechanisms driving metabolite exposure. A top-down approach is typically favored when there are clinical metabolite concentration time data available; however, the middle-out approach is considered the most mechanistically relevant.

are the only examples where the interaction potential of parent alone does not translate to a positive DDI observed in the clinic. However, the major circulating metabolites of these drugs inhibit enzymes and transporters *in vitro*, which could explain the disconnect.[12] We evaluated these drugs (amiodarone, gemfibrozil, and sertraline) using PBPK modeling to mechanistically understand the quantitative contribution of the metabolites to the DDIs; additionally, we reviewed the literature for other examples of metabolite-precipitated DDIs (**Supplemental Table 2**). Some common themes emerged across the three case studies reviewed. First, PBPK models were used to quantitatively rationalize and support the observed DDI via exploring inhibition mechanisms of both parent and metabolite. Second, all case studies presented in this work utilized both *in vitro* and observed clinical pharmacokinetic data of metabolites in order to build and verify model parameters for metabolites, through a "middle-out" approach. Third, uncertainty in model verification and quantitative prediction increase when multiple metabolites are involved. And finally, true prospective prediction ("bottom-up" modeling) of metabolite-mediated DDI can be challenging due to the uncertainty associated with the prediction of *in vivo* disposition of metabolites. Consistent with this assessment, many of the recent published examples of mechanistic modeling to assess metabolite mediated DDIs adopted a "middle-out" approach (**Supplementary Table 2**). Nevertheless, approaches for developing "bottom-up" PBPK models to predict metabolite exposure using the *in vitro* data have been described and can be applied for prospective predictions.[70]

Based on our learnings from the exercise and considering the literature examples, we believe that the following stage-wise strategy (**Figure 3**) will be useful for the application of PBPK modeling and simulation to improve understanding of the potential contribution of inhibitory metabolites to clinical DDIs. In scenarios where metabolite contribution to DDI is suspected, *in vivo* metabolite exposure data can be used to support initial predictions based on the mechanistic

static model. In the absence of *in vivo* metabolite exposure data, a PBPK model must be developed based on *in vitro* metabolite formation and elimination rates determined *in vitro*. Such "bottom-up" models may be verified when the *in vivo exposure* data are available. In either scenario, a verified PBPK model for the parent provides more confidence in the utility of the metabolite PBPK model.

The case studies described here demonstrate the utility of the PBPK approach as a tool to quantitatively rationalize the underlying mechanisms of DDI involving inhibitory metabolites. Furthermore, this approach provides insights for prospective prediction of DDIs. Prospective DDI prediction involving metabolites can be accomplished through the integration of the disposition kinetics of both parent and metabolite, and the *in vitro* interaction potency of each. The prediction of metabolite pharmacokinetics in human may be heavily based on *in vitro* or preclinical (animal) data, and therefore, there is a need to build confidence in the exposure projection of the metabolite(s).[45,71] Prospective investigations will typically be triggered in response to specific clues.[12,71] These include scenarios in which parent drug is a potent inhibitor, or where metabolites are projected to circulate systemically at concentrations equal to or exceeding parent after multiple doses.[12] Yu *et al*. concluded that it is important to consider inhibition potential of metabolite whenever parent is likely to inhibit CYPs.[12] However, only abundant metabolites should be considered for investigation *in vitro* when parent is not likely to inhibit CYPs. In response to these clues, suspected inhibitory metabolites must then be tested in multiple *in vitro* systems (including a panel of drug metabolizing enzymes and transporters). Furthermore, disposition attributes of the metabolites should be investigated in a similar manner as the parent drug so as to provide relevant inputs for the PBPK modeling.[45]

In prospective PBPK model building, considerable uncertainty is associated with the pharmacokinetics of both parent and inhibitory metabolite. At this stage, sensitivity analyses are highly recommended in order to predict a range of likelihood for the simulated interaction magnitude and to address fit-for-purpose questions at decision points. Model parameter optimization is recommended as the clinical data become available. For example, parameter optimization relevance may be evaluated through verification of pharmacokinetic profiles for both parent and metabolite, when both single- and multiple-dose clinical data become available. However, any optimization steps must be based on a sound mechanistic understanding of parent and metabolite disposition *in vivo*.

Although PBPK is a better mechanistic approach, in particular scenarios, static models can be considered.[72] Depending on the pharmacokinetic profile of parent and metabolite, the prediction from static and PBPK approaches will often be different due to the manner in which inhibitor concentration is described by each model (static vs. dynamic). However, predictions of the static model serve as a useful reference for evaluating and troubleshooting the PBPK model, which will provide higher confidence in the predictions. The static models will generally be useful during early development stages, such as clinical candidate nomination, when extensive clinical metabolite data are not available. However, estimates of inhibitory potency, clinically relevant inhibitor concentration, and protein binding ($f_{u,p}$, $f_{u,mic}$) for both parent and metabolite must be accurately determined/projected in order to generate useful DDI predictions.

CONCLUSION

Based on the collection of our work, it can be said that PBPK modeling provides mechanistic understanding for the observed clinical DDI caused by inhibitory metabolite(s). However, a true prospective prediction of DDIs involving major circulating inhibitory metabolites is challenging, primarily due to uncertainty associated with complex metabolite disposition pathways leading to low confidence in projecting metabolite exposure. Therefore, we recommend a stage-wise modeling approach. Static models should generally be applied in early development when limited data are available. PBPK models will be useful particularly in the later stages of development, based on the availability of *in vitro* and *in vivo* metabolite data. Confidence in model predictions will increase with full validation of the metabolite model as more *in vivo* data become available. Overall, PBPK modeling is a useful tool to quantitatively rationalize observed drug interactions and understand the underlying mechanisms including the contribution of perpetrator metabolites.

Acknowledgments. This article represents collaborative efforts of representatives of DMLG member companies, including Grant Generaux and Chris MacLauchlin (formerly of GlaxoSmithKline), Edgar L. Schuck (Eisai), Susanna Tse (Pfizer), Chuang Lu (Millennium), and Guanfa Gan and Jin Zhou (Boehringer Ingelheim).

Conflict of Interest. The authors declare no conflicts of interest.

1. Kirch W, *et al.* Cisapride-cimetidine interaction: enhanced cisapride bioavailability and accelerated cimetidine absorption. *Ther. Drug Monit.* **11**, 411–414 (1989).
2. Leape LL, *et al.* Systems analysis of adverse drug events. ADE Prevention Study Group. *JAMA* **274**, 35–43 (1995).
3. Monahan BP, *et al.* Torsades de pointes occurring in association with terfenadine use. *JAMA* **264**, 2788–2790 (1990).
4. Fahmi OA, *et al.* A combined model for predicting CYP3A4 clinical net drug-drug interaction based on CYP3A4 inhibition, inactivation, and induction determined in vitro. *Drug Metab. Dispos.* **36**, 1698–1708 (2008).
5. Chu X, *et al.* Intracellular drug concentrations and transporters: measurement, modeling, and implications for the liver. *Clin. Pharmacol. Ther.* **94**, 126–141 (2013).
6. Konig J, *et al.* Transporters and drug-drug interactions: important determinants of drug disposition and effects. *Pharmacol. Rev.* **65**, 944–966 (2013).
7. Tweedie D, *et al.* Transporter studies in drug development: experience to date and follow-up on decision trees from the International Transporter Consortium. *Clin. Pharmacol. Ther.* **94**, 113–125 (2013).
8. Zamek-Gliszczynski MJ, *et al.* ITC recommendations for transporter kinetic parameter estimation and translational modeling of transport-mediated PK and DDIs in humans. *Clin. Pharmacol. Ther.* **94**, 64–79 (2013).
9. Yeung CK, *et al.* Are circulating metabolites important in drug-drug interactions? Quantitative analysis of risk prediction and inhibitory potency. *Clin. Pharmacol. Ther.* **89**, 105–113 (2011).
10. Lutz JD, *et al.* Stereoselective inhibition of CYP2C19 and CYP3A4 by fluoxetine and its metabolite: implications for risk assessment of multiple time-dependent inhibitor systems. *Drug Metab. Dispos.* **41**, 2056–2065 (2013).
11. Templeton IE, *et al.* Contribution of itraconazole metabolites to inhibition of CYP3A4 in vivo. *Clin. Pharmacol. Ther.* **83**, 77–85 (2008).

12. Yu H, *et al*. Contribution of metabolites to P450 inhibition-based drug-drug interactions: scholarship from the drug metabolism leadership group of the innovation and quality consortium metabolite group. *Drug Metab. Dispos.* **43**, 620–630 (2015).
13. Yu H, *et al*. A perspective on the contribution of metabolites to drug-drug interaction potential: the need to consider both circulating levels and inhibition potency. *Drug Metab. Dispos.* **41**, 536–540 (2013).
14. FDA. Drug Interaction Studies—Study Design, Data Analysis, Implications for Dosing, and Labeling Recommendations DRAFT GUIDANCE. In: Center for Drug Evaluation and Research CP, editor. February 2012 ed. <druginfo@fda.hhs.gov> (2012).
15. EMA. Guideline on the investigation of drug interactions. <http://www.ema.europa.eu/docs/en_GB/document_library/Scientific_guideline/2012/07/WC500129606.pdf> (2012).
16. Jones HM, *et al*. Physiologically based pharmacokinetic modeling in drug discovery and development: a pharmaceutical industry perspective. *Clin. Pharmacol. Ther.* **97**, 247–262 (2015).
17. Lutz JD, *et al*. Rationalization and prediction of in vivo metabolite exposures: the role of metabolite kinetics, clearance predictions and in vitro parameters. *Expert Opin. Drug Metab. Toxicol.* **6**, 1095–1109 (2010).
18. Rowland M, *et al*. *Clinical Pharmacokinetics: Concepts and Applications* (Philadelphia, Williams & Wilkins, 1995).
19. Lin JH, *et al*. Is the role of the small intestine in first-pass metabolism overemphasized? *Pharmacol. Rev.* **51**, 135–157 (1999).
20. Paine MF, *et al*. The human intestinal cytochrome P450 "pie." *Drug Metab. Dispos.* **34**, 880–886 (2006).
21. Paine MF, *et al*. Characterization of interintestinal and intraintestinal variations in human CYP3A-dependent metabolism. *J Pharmacol. Exp. Ther.* **283**, 1552–1562 (1997).
22. Kolars JC, *et al*. First-pass metabolism of cyclosporin by the gut. *Lancet* **338**, 1488–1490 (1991).
23. Paine MF, *et al*. First-pass metabolism of midazolam by the human intestine. *Clin. Pharmacol. Ther.* **60**, 14–24 (1996).
24. Thummel KE, *et al*. Oral first-pass elimination of midazolam involves both gastrointestinal and hepatic CYP3A-mediated metabolism. *Clin. Pharmacol. Ther.* **59**, 491–502 (1996).
25. von Richter O, *et al*. Determination of in vivo absorption, metabolism, and transport of drugs by the human intestinal wall and liver with a novel perfusion technique. *Clin. Pharmacol. Ther.* **70**, 217–227 (2001).
26. Gertz M, *et al*. Prediction of human intestinal first-pass metabolism of 25 CYP3A substrates from in vitro clearance and permeability data. *Drug Metab. Dispos.* **38**, 1147–1158 (2010).
27. Loi CM, *et al*. Which metabolites circulate? *Drug Metab. Dispos.* **41**, 933–951 (2013).
28. International Transporter C, *et al*. Membrane transporters in drug development. *Nat. Rev. Drug Discov.* **9**, 215–236 (2010).
29. Berggren S, *et al*. Regional transport and metabolism of ropivacaine and its CYP3A4 metabolite PPX in human intestine. *J. Pharm. Pharmacol.* **55**, 963–972 (2003).
30. Kimoto E, *et al*. Hepatic disposition of gemfibrozil and its major metabolite, gemfibrozil 1-O-beta-glucuronide. *Mol. Pharm.* (2015).
31. Varma MV, *et al*. Quantitative rationalization of gemfibrozil drug interactions: consideration of transporters-enzyme interplay and the role of circulating metabolite gemfibrozil 1-O-beta-glucuronide. *Drug Metab. Dispos.* **43**, 1108–1118 (2015).
32. Ito K, *et al*. Database analyses for the prediction of in vivo drug-drug interactions from in vitro data. *Br. J. Clin. Pharmacol.* **57**, 473–486 (2004).
33. Obach RS, *et al*. Mechanism-based inactivation of human cytochrome p450 enzymes and the prediction of drug-drug interactions. *Drug Metab. Dispos.* **35**, 246–255 (2007).
34. Kirby BJ, *et al*. Complex drug interactions of HIV protease inhibitors 1: inactivation, induction, and inhibition of cytochrome P450 3A by ritonavir or nelfinavir. *Drug Metab. Dispos.* **39**, 1070–1078 (2011).
35. Obach RS, *et al*. The utility of in vitro cytochrome P450 inhibition data in the prediction of drug-drug interactions. *J. Pharmacol. Exp. Ther.* **316**, 336–348 (2006).
36. Templeton I, *et al*. Accurate prediction of dose-dependent CYP3A4 inhibition by itraconazole and its metabolites from in vitro inhibition data. *Clin. Pharmacol. Ther.* **88**, 499–505 (2010).
37. Varma MV, *et al*. Quantitative prediction of transporter- and enzyme-mediated clinical drug-drug interactions of organic anion-transporting polypeptide 1B1 substrates using a mechanistic net-effect model. *J. Pharmacol. Exp. Ther.* **351**, 214–223 (2014).
38. Varma MV, *et al*. Quantitative prediction of repaglinide-rifampicin complex drug interactions using dynamic and static mechanistic models: delineating differential CYP3A4 induction and OATP1B1 inhibition potential of rifampicin. *Drug Metab. Dispos.* **41**, 966–974 (2013).
39. Rowland M, *et al*. Kinetics of drug-drug interactions. *J. Pharmacokinet. Biopharm.* **1**, 553–567 (1973).
40. Wang YH, *et al*. Prediction of cytochrome P450 3A inhibition by verapamil enantiomers and their metabolites. *Drug Metab. Dispos.* **32**, 259–266 (2004).
41. Yang J, *et al*. Prediction of intestinal first-pass drug metabolism. *Curr. Drug Metab.* **8**, 676–684 (2007).
42. Bohnert T, *et al*. Evaluation of a new molecular entity as a victim of metabolic drug-drug interactions — an industry perspective. *Drug Metab. Dispos.* e-pub ahead of print 2016.
43. Rostami-Hodjegan A, *et al*. 'In silico' simulations to assess the 'in vivo' consequences of 'in vitro' metabolic drug-drug interactions. *Drug Discov. Today Technol.* **1**, 441–448 (2004).
44. Zhao P, *et al*. Applications of physiologically based pharmacokinetic (PBPK) modeling and simulation during regulatory review. *Clin. Pharmacol. Ther.* **89**, 259–267 (2011).
45. Zhao P, *et al*. Best practice in the use of physiologically based pharmacokinetic modeling and simulation to address clinical pharmacology regulatory questions. *Clin. Pharmacol. Ther.* **92**, 17–20 (2012).
46. Chen Y, *et al*. Physiologically based pharmacokinetic modeling to predict drug-drug interactions involving inhibitory metabolite: a case study of amiodarone. *Drug Metab. Dispos.* **43**, 182–189 (2015).
47. Heimark LD, *et al*. The mechanism of the interaction between amiodarone and warfarin in humans. *Clin. Pharmacol. Ther.* **51**, 398–407 (1992).
48. Werner D, *et al*. Effect of amiodarone on the plasma levels of metoprolol. *Am. J. Cardiol.* **94**, 1319–1321 (2004).
49. Becquemont L, *et al*. Amiodarone interacts with simvastatin but not with pravastatin disposition kinetics. *Clin. Pharmacol. Ther.* **81**, 679–684 (2007).
50. Ohyama K, *et al*. Inhibitory effects of amiodarone and its N-deethylated metabolite on human cytochrome P450 activities: prediction of in vivo drug interactions. *Br. J. Clin. Pharmacol.* **49**, 244–253 (2000).
51. McDonald MG, *et al*. Warfarin-amiodarone drug-drug interactions: determination of [I](u)/K(I,u) for amiodarone and its plasma metabolites. *Clin. Pharmacol. Ther.* **91**, 709–717 (2012).
52. Holt DW, *et al*. Amiodarone pharmacokinetics. *Am. Heart J.* **106**, 840–847 (1983).
53. Spencer CM, *et al*. Gemfibrozil. A reappraisal of its pharmacological properties and place in the management of dyslipidaemia. *Drugs* **51**, 982–1018 (1996).
54. Farmer JA. Learning from the cerivastatin experience. *Lancet* **358**, 1383–1385 (2001).
55. Backman JT, *et al*. Gemfibrozil greatly increases plasma concentrations of cerivastatin. *Clin. Pharmacol. Ther.* **72**, 685–691 (2002).
56. Honkalammi J, *et al*. Dose-dependent interaction between gemfibrozil and repaglinide in humans: strong inhibition of CYP2C8 with subtherapeutic gemfibrozil doses. *Drug Metab. Dispos.* **39**, 1977–1986 (2011).
57. Niemi M, *et al*. Effects of gemfibrozil, itraconazole, and their combination on the pharmacokinetics and pharmacodynamics of repaglinide: potentially hazardous interaction between gemfibrozil and repaglinide. *Diabetologia* **46**, 347–351 (2003).
58. Aquilante CL, *et al*. Impact of the CYP2C8 *3 polymorphism on the drug-drug interaction between gemfibrozil and pioglitazone. *Br. J. Clin. Pharmacol.* **75**, 217–226 (2013).
59. Niemi M, *et al*. Gemfibrozil considerably increases the plasma concentrations of rosiglitazone. *Diabetologia* **46**, 1319–1323 (2003).
60. Shitara Y, *et al*. Gemfibrozil and its glucuronide inhibit the organic anion transporting polypeptide 2 (OATP2/OATP1B1:SLC21A6)-mediated hepatic uptake and CYP2C8-mediated metabolism of cerivastatin: analysis of the mechanism of the clinically relevant drug-drug interaction between cerivastatin and gemfibrozil. *J. Pharmacol. Exp. Ther.* **311**, 228–236 (2004).
61. Fujino H, *et al*. Studies on the interaction between fibrates and statins using human hepatic microsomes. *Arzneimittelforschung* **53**, 701–707 (2003).
62. Ogilvie BW, *et al*. Glucuronidation converts gemfibrozil to a potent, metabolism-dependent inhibitor of CYP2C8: implications for drug-drug interactions. *Drug Metab. Dispos.* **34**, 191–197 (2006).
63. Kobayashi K, *et al*. Sertraline N-demethylation is catalyzed by multiple isoforms of human cytochrome P-450 in vitro. *Drug Metab. Dispos.* **27**, 763–766 (1999).
64. Obach RS, *et al*. Sertraline is metabolized by multiple cytochrome P450 enzymes, monoamine oxidases, and glucuronyl transferases in human: an in vitro study. *Drug Metab. Dispos.* **33**, 262–270 (2005).
65. Wang JH, *et al*. Pharmacokinetics of sertraline in relation to genetic polymorphism of CYP2C19. *Clin. Pharmacol. Ther.* **70**, 42–47 (2001).
66. Kurtz DL, *et al*. The effect of sertraline on the pharmacokinetics of desipramine and imipramine. *Clin. Pharmacol. Ther.* **62**, 145–156 (1997).
67. Alderman J. Coadministration of sertraline with cisapride or pimozide: an open-label, nonrandomized examination of pharmacokinetics and corrected QT intervals in healthy adult volunteers. *Clin. Ther.* **27**, 1050–1063 (2005).
68. Desta Z, *et al*. Identification and characterization of human cytochrome P450 isoforms interacting with pimozide. *J. Pharmacol. Exp. Ther.* **285**, 428–437 (1998).
69. Desta Z, *et al*. Effect of clarithromycin on the pharmacokinetics and pharmacodynamics of pimozide in healthy poor and extensive metabolizers of cytochrome P450 2D6 (CYP2D6). *Clin. Pharmacol. Ther.* **65**, 10–20 (1999).
70. Nguyen HQ, *et al*. Mechanistic modeling to predict midazolam metabolite exposure from in vitro data. *Drug Metab. Dispos.* e-pub ahead of print 2016.
71. Callegari E, *et al*. Drug metabolites as cytochrome p450 inhibitors: a retrospective analysis and proposed algorithm for evaluation of the pharmacokinetic interaction

potential of metabolites in drug discovery and development. *Drug Metab. Dispos.* **41**, 2047–2055 (2013).
72. Peters SA, *et al*. Evaluation of the use of static and dynamic models to predict drug-drug interaction and its associated variability: impact on drug discovery and early development. *Drug Metab. Dispos.* **40**, 1495–1507 (2012).

Supplementary information accompanies this paper on the *CPT: Pharmacometrics & Systems Pharmacology* website (http://www.wileyonlinelibrary.com/psp4)